

Experimental Techniques for Mechanical Characterization of Hydrogels at the Microscale

by B. Johnson, J.M. Bauer, D.J. Niedermaier, W.C. Crone and D.J. Beebe

ABSTRACT—Hydrogel actuators in microfluidic devices must endure the forces of aqueous flow, the constraint of device walls, and the restoring force of elastic membranes. In order to assess the capabilities of hydrogels, three experimental techniques for determining the uniaxial tensile properties and functional swelling properties of microscale hydrogel structures have been developed. Tensile tests were conducted to determine Young's modulus and Poisson's ratio at varying degrees of swelling equilibrium. Force response tests were performed to determine the force exerted by cylindrical hydrogel structures on compression platens held at fixed displacement. Particle image velocimetry, a method originally developed to measure velocity fields in fluid flows, was adapted to investigate the deformation rates at various times within hydrogel structures during volumetric swelling. The techniques and sample fabrication methods outlined are applicable to a variety of hydrogel chemistries.

KEY WORDS—Mechanical properties, PIV, hydrogel, active materials

Introduction

Hydrogels with volumetric shape memory capability are now being employed as actuators,¹ fluid pumps,² and valves¹ in microfluidic devices. Although the properties of hydrogels are similar to soft biological materials, they can be employed much like muscles and tendons in engineering devices. In an aqueous environment, hydrogels will undergo a reversible phase transformation that results in dramatic volumetric swelling and shrinking upon exposure and removal of a stimulus. Hydrogels have been produced that actuate when exposed to such stimuli as pH,³ salinity,⁴ electrical current,⁵ temperature,⁶ and antigens.⁷ Since the rate of swelling and shrinking in a hydrogel is diffusion-limited, the temporal response of macroscale hydrogel structures can be reduced to minutes or even seconds by reducing the size scale of the device.⁸

Our research considers a poly(2-hydroxyethyl methacrylate) (HEMA) gel which incorporates an ethyleneglycol-dimethacrylate (EGDMA) crosslinker, 2,2-dimethoxy-2-phenyl-acetophenone (DMPA) photoinitiator, and acrylic acid (AA) co-monomer that is pH sensitive. The resulting gel is sensitive to the pH of its aqueous environment; expanding at high pH and shrinking at low pH (Fig. 1). This hydrogel has been applied to the autonomous control of flow in microfluidic devices.⁸ Understanding the mechanical behavior of this hydrogel is important to both the design of devices, and the modeling of hydrogel behavior. The mechanical properties of the hydrogels are critical to device design because in actuation applications the gels must endure forces imposed by the flow of an aqueous solution, the constraint of device walls during swelling, and the restoring force of elastic membranes.⁹ Additionally, there is a strong desire to better understand the underlying mechanisms for swelling in hydrogels so that more predictive models can be developed to guide the design process.

A number of researchers have reported on studies of the mechanical properties of hydrogels.^{10–16} The specific test protocols of these studies often vary since it is necessary to test hydrogels within the context of their intended applications (e.g. artificial tissue replacements for ligaments,¹⁰ muscles,¹⁵ and cartilage.¹⁶) Although compressive tests may provide valuable insight into the functional behavior of hydrogels,¹⁶ several studies have employed this methodology to determine material properties such as the Young's modulus.^{14,17,18} However, the accuracy of modulus measurements from compression tests may be compromised by friction that restricts the Poisson effect in cylindrical samples of small length to diameter ratios ($L/d \leq 1$)¹⁹ Additionally, if L/d is large, buckling may introduce inaccuracies, again making modulus measurements collected with compression testing undesirable.

Our techniques have addressed the macroscopic uniaxial tensile properties in addition to the functional swelling properties (force generation and deformation rate) of hydrogel structures in microchannels. Tensile testing was used for all modulus measurements while compression and constrained testing were reserved for force response and swelling measurements. Testing these materials poses some unique challenges as well as unique opportunities. Several testing techniques that can be used to characterize shape memory hydrogels are reviewed. Critical to the success of these techniques is the ability to polymerize hydrogels into specific shapes with embedded beads that can be used to track displacement during deformation and volumetric expansion.

B. Johnson is a graduate student and D.J. Beebe is an Associate Professor, Department of Biomedical Engineering, University of Wisconsin-Madison, Madison, WI 53706, USA. D.J. Niedermaier is a Research Assistant, University of Wisconsin-Madison, Engineering Mechanics Program, Madison, WI 53706, USA. J.M. Bauer is a graduate student, Beckman Institute for Advanced Science and Technology, University of Illinois at Urbana-Champaign, Urbana, IL 6181, USA. W.C. Crone (crone@engr.wisc.edu) (SEM member) is an Assistant Professor, Department of Biomedical Engineering, the Engineering Mechanics Program, and the Department of Engineering Physics, University of Wisconsin-Madison, Madison, WI 53706, USA.

Original manuscript submitted: April 30, 2002.

Final manuscript received: March 30, 2003.

DOI: 10.1177/0014485104039629

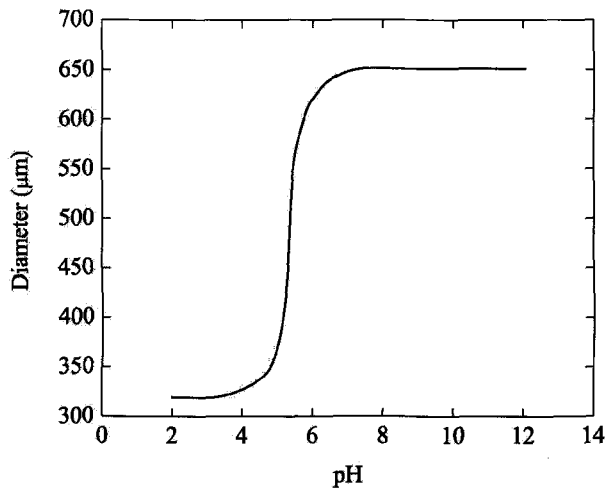


Fig. 1—Discontinuous swelling behavior of a hydrogel sensitive to environmental pH. The plot was adapted from experimental data presented in De et al.,²³ where the diameters of cylindrical hydrogel structures were measured in a microchannel at different levels of pH equilibrium

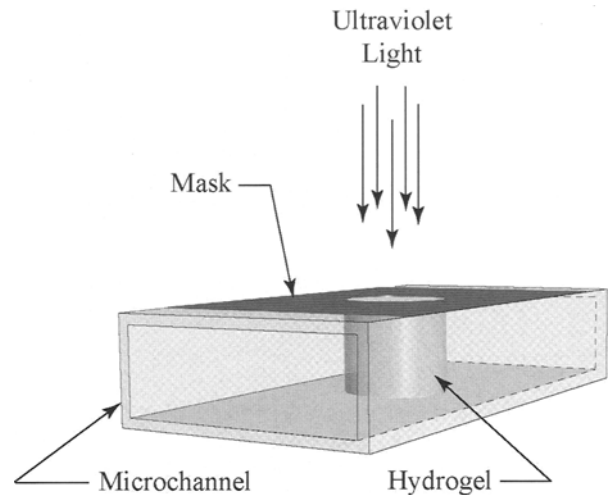


Fig. 2—In situ photopolymerization of a hydrogel cylinder in a microchannel

Sample Preparation

Test samples of HEMA gel are created by polymerization from a liquid prepolymer mixture using ultraviolet (UV) light. A variety of sample structures can be created by using either masking or casting techniques. *In situ* photopolymerization techniques, used in the creation of microvalve actuators in microchannels,⁸ employ a mask to create a structure inside a channel or between two rigid plates (Fig. 2). Prepolymer mixture is introduced into the channel while a mask is placed over the channel. The transparent image of the shape to be polymerized is positioned over the channel and a UV source is used to polymerize the prepolymer mixture below the image. The unpolymerized liquid is flushed from the channel using solutions of methanol and deionized water. The top of the channel can also be removed after polymerization for tests requiring direct contact with the gel. This method has been used to create samples for both the force response testing and the particle image velocimetry (PIV) experiments described below. It is, however, limited by optical and diffusion effects that arise during the polymerization of larger samples, in which non-rectilinear cross-sectional geometries result.

An alternative preparation procedure for larger samples, involving a polydimethylsiloxane (PDMS) mold, can be used to cast individual samples like those shown schematically in Fig. 3.²⁰ The advantage of this technique is that multiple uniform samples can be produced with rectilinear cross-sectional geometries and minimal waste of the prepolymer mixture. The multilayered mold was prepared by first patterning negative-tone UV photoresist on a silicon wafer, followed by a compression molding process to produce a PDMS stencil.²¹ The resulting stencil was placed on a layer of PDMS, coated with a surfactant solution, and covered with a third layer of PDMS after the prepolymer mixture was injected into the mold. Polymerization took place under a Novacure UV source that delivered UV light at an intensity of

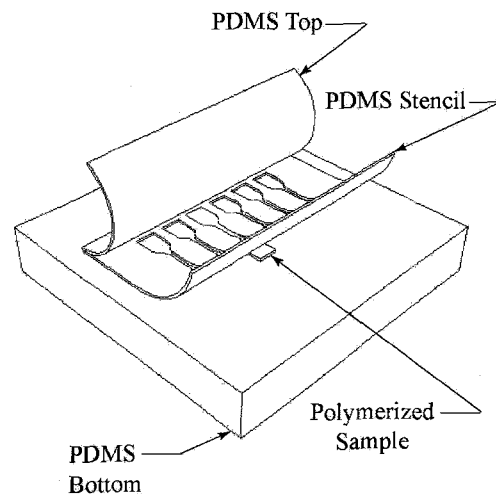


Fig. 3—PDMS mold used in the fabrication of tensile samples. The casting process produced dumbbell-shaped structures with a 5.5 mm gage length, 1 mm neck width, and approximate thicknesses of 200 and 500 μm for the elastic modulus and the Poisson ratio experiments, respectively

15 mW cm⁻² for 2 min. After the samples were removed from the mold, they were washed with methanol and deionized water and stored in a buffered pH solution. Samples were allowed to equilibrate for at least 24 h prior to tensile testing.

Testing Techniques and Experimental Results

Tensile Testing

Mechanical properties such as Young's modulus, the Poisson ratio, and ultimate strength are of interest in model development^{22,23} An Instron Model 5548 MicroTester, equipped with a 10 N load cell, was used for measuring the mechanical properties of hydrogel tensile samples. The type

IV sample size suggested by ASTM D 638-99²⁴ was scaled down to a gage section width of 1 mm to better approximate the size of components used in microfluidic devices. The position of the screw-driven actuator could be determined to within $\pm 6.0 \mu\text{m}$ over 100 mm of travel, while loads could be measured to within $\pm 0.25\%$ of the indicated force. This level of accuracy is required for the small and flexible hydrogel samples that were tested.

Testing must also be conducted under controlled environmental conditions in an aqueous solution. The custom bath and grips shown in Fig. 4 were constructed to handle potentially corrosive buffer solutions with controlled pH and temperature. The walls of the bath were constructed from transparent material to allow for image acquisition during testing. The inner glass cylinder holds the pH solution, which can be removed and replaced through ports in the bottom of the chamber. The outer cylinder, made of PMMA, holds a temperature controlled water bath that circulates through ports in the outer wall of the cylinder. The grip fixtures were machined from acrylic. Self-aligning grip faces were clamped to the sample by a screw-tightened mechanism. Fine grit sandpaper was affixed to the grip faces to prevent sample slippage.

Due to the limited mechanical strength of hydrogels and the aqueous environment in which they must be tested, the use of an extensometer is not a feasible means for measuring strains in the material. Utilizing crosshead displacements to determine axial strains is generally adequate; however, transverse strains are also needed for the determination of the Poisson ratio. Because the samples are polymerized from a liquid state, it is possible to mix beads with the prepolymer solution so that a random array of particles can be polymerized in the gel and tracked optically. Small glass beads of approximately $30 \mu\text{m}$ diameter were used to track deformation during tensile testing. It has been assumed that the beads do not significantly affect the macroscopic material properties of the hydrogel since they occupy much less than 0.1% of the volume of the gage section and the bead diameter is less than 6% of the smallest specimen length scale. The embedded beads were used in conjunction with a CCD camera, frame grabber, personal computer equipped with image analysis software (MetaMorph version 4.6r6), light source, and a cylindrical lens placed between the camera lens and environmental chamber to provide in-plane strain data. Sequential still images were captured throughout the course of the tension test such that axial and transverse strains could be determined from the bead positions.

A constant crosshead displacement rate of 5 mm min^{-1} was used to determine the tensile properties of the hydrogel as a function of solution pH. The test rate of 5 mm min^{-1} was chosen because it produced rupture in the sample within the time frame (1/2 to 5 min) suggested by ASTM D 638-99.²⁴ The pH solution was held at a constant temperature of $24 \pm 1^\circ\text{C}$. Cross-sectional areas for stress calculations were measured with an optical microscope and Metamorph software after each test was completed. Representative stress-strain data are shown in Fig. 5 for samples tested to failure at three pH levels. A comprehensive investigation into the effects of solution pH on the elastic modulus has been reported elsewhere.^{20,25} Young's modulus was calculated from the slope of the stress-strain curve within the region of 10% strain (inset of Fig. 5). The resulting moduli were found to be 0.32 ± 0.01 , 0.24 ± 0.03 , and $0.16 \pm 0.03 \text{ MPa}$ for samples tested in solutions of pH 2.9, 5.5, and 12, respectively.

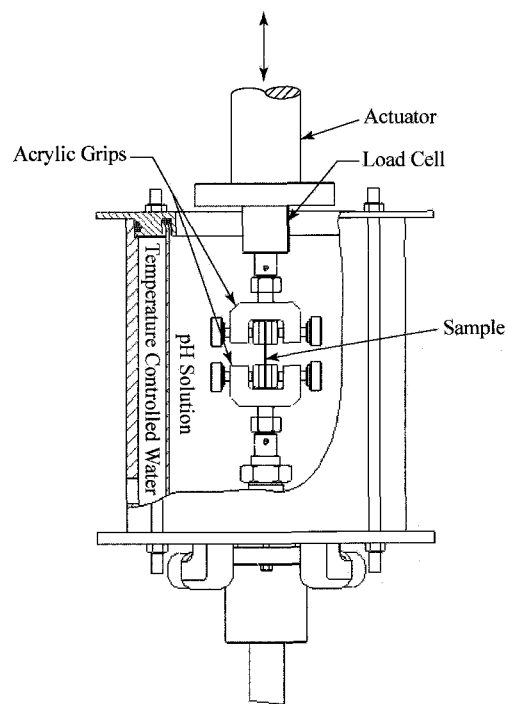


Fig. 4—Environmental chamber and sample/grip assembly

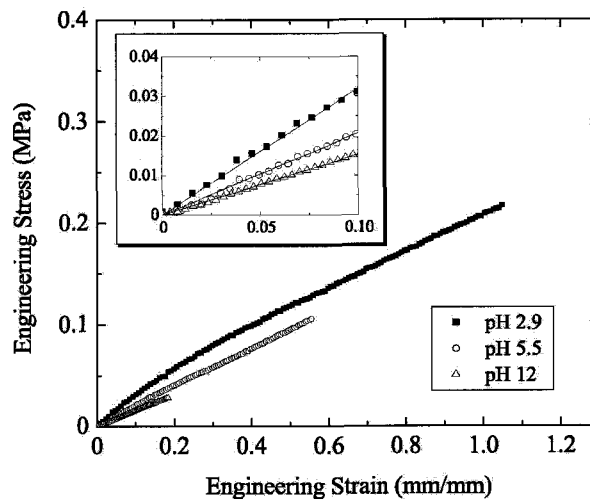


Fig. 5—The graph shows the stress-strain relationship of hydrogel samples tested at three pH levels. The Young's modulus was calculated from the slope of the stress-strain curve within the region of 10% strain (see inset), where axial strains were determined from crosshead position

It is evident from Fig. 5 that the ultimate strength as well as the strain required to fracture the hydrogel sample decrease significantly with increasing pH (swelling).

The Poisson ratio experiments were conducted at a displacement rate of 2 mm min^{-1} in order to accommodate limitations in the optical setup. Specifically, the reduction in test rate was required because the intensity of light reflected off the glass beads diminished upon passage through opti-

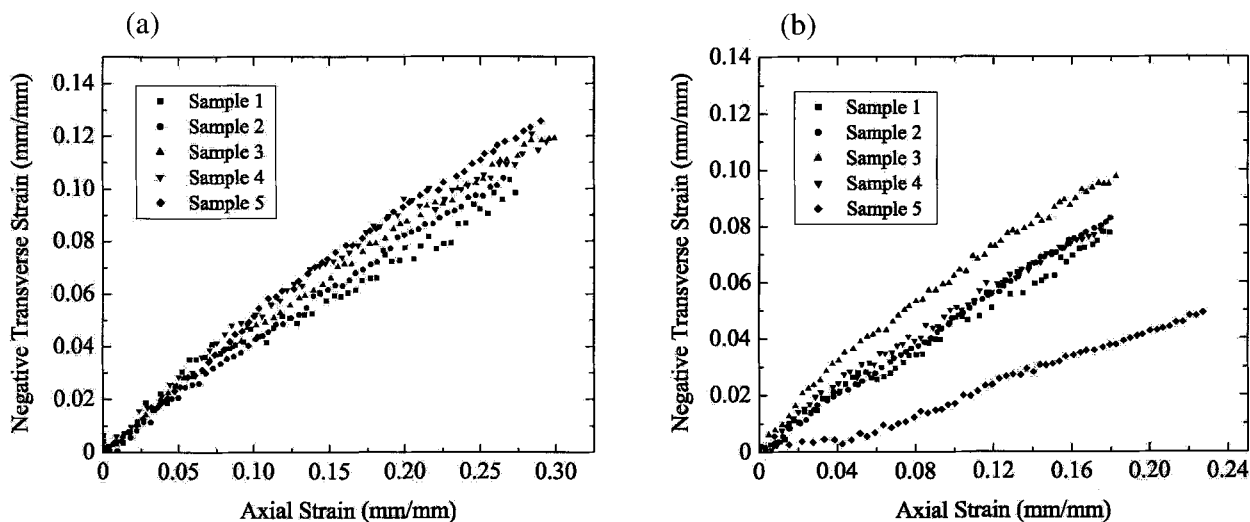


Fig. 6—(a) Transverse and axial strain data for five samples tested in a phosphate buffer solution of pH 2.8. (b) Similar data illustrate the reduced repeatability of strain measurements for samples tested in their swollen state at pH 12

cal components (lenses and bath walls) and the surrounding media (pH buffer and water). This required longer exposure times, which in turn limited the maximum frequency of image acquisition. Therefore, the displacement rate was decreased such that an adequate number of images could be acquired before the beads of interest traveled out of the field of view (approximately $6.2 \times 4.5 \text{ mm}^2$) of the camera. Figures 6(a) and 6(b) show the resulting biaxial strain data for a set of five samples tested at two different pH levels. The Poisson ratio was determined to be 0.42 ± 0.03 at pH 2.8 and 0.45 ± 0.12 at pH 12. The scatter observed in the pH 12 dataset will be discussed below.

Several experiments were conducted to verify the accuracy of the strains determined from crosshead displacements and the negligible influence of the slightly different strain rates used. Strains calculated from crosshead displacement consistently slightly overestimated the strains calculated from optical observation of the bead position. For example, a test performed on a 19 mm gage length sample produced crosshead strains of only 1.4% greater than bead strains over a range of 3.6–10%. Thus, the effect on modulus calculated from crosshead strains is negligible. Furthermore, comparative tests were conducted at the two strain rates utilized (2 and 5 mm min^{-1}). Although hydrogels are inherently viscoelastic, differences in moduli measured at these two rates are negligible.

Force Response Testing

A critical parameter of interest for the design of microfluidic devices is the amount of force the hydrogel is capable of exerting during swelling. For example, numerous pump and valve designs incorporate membranes that must be depressed by an actuating cylindrical hydrogel in order to control fluid flow.^{9,26} Additionally, forces acting on stationary channel walls must be controlled to avoid delamination and regulate frictional interactions. Thus, quantification of the magnitude and response time of the force produced by a hydrogel actuator during the swelling process is of critical importance to the effort of device optimization.

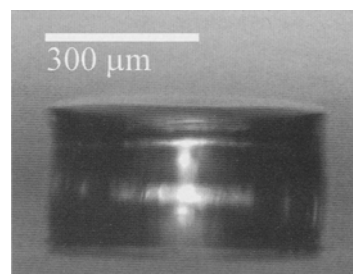


Fig. 7—Optical image (side view) of a hydrogel used in force response tests. The cylinder has an approximate diameter of $600 \mu\text{m}$ and height of $300 \mu\text{m}$

The test was configured in a manner that would mimic the conditions of a channel in a microfluidic device. The Instron MicroTester was equipped with a 50 mm diameter stainless-steel compression platen that supported a shallow glass dish filled with buffered pH solution. A custom-built acrylic compression platen (6.35 mm diameter) was connected to a 10 N load cell and served as an analogue to the upper wall of a microchannel.

A cylindrical hydrogel structure, $600 \mu\text{m}$ in diameter, was polymerized on a glass substrate by using a similar masking technique to that described above. Instead of a permanent channel top, however, a removable non-adherent plastic sheet was used. After polymerization, the mask and non-adherent sheet were peeled back leaving the hydrogel cylinder on a glass substrate surrounded by PDMS sidewalls. Figure 7 shows a side view of a typical test specimen. The sample was dried and kept in air for storage prior to testing. Prolonged hydration had a negative effect on adhesion to the glass substrate.

For testing, the hydrogel was placed in the glass dish and the upper compression platen was manually lowered onto the top surface of the surrounding PDMS sidewalls. Although

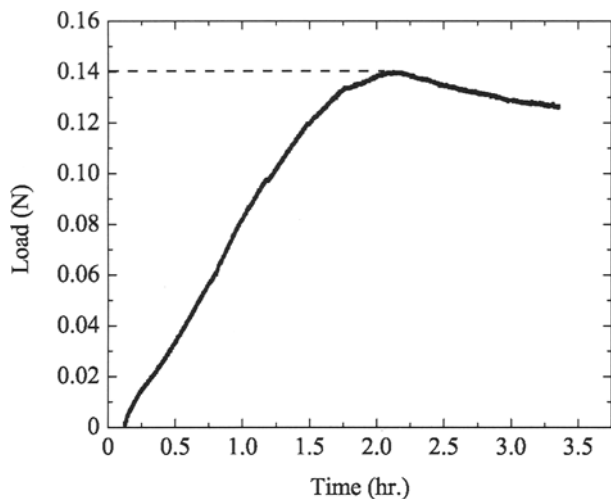


Fig. 8—Typical force response curve generated by a 600 μm hydrogel structure swelling in pH 12 buffer. The hydrogel exerted a maximum force of 0.14 N on the upper platen of the test machine after approximately 2.1 h of swelling

contact with the sample may not occur during this procedure, the distance between the top platen and the glass substrate were kept constant. After a buffered pH solution was poured into the glass dish, the load cell was reset to account for buoyancy effects on the platen. Load data were acquired over time while holding the displacement constant. A typical force response curve for a 600 μm diameter sample is shown in Fig. 8. A hydrogel of this size is capable of exerting 0.14 N on the upper platen of the test machine after approximately 2.1 h of swelling. This is significantly greater than forces generated by similar sized microelectromechanical systems (MEMS) actuators.²⁷

Particle Image Velocimetry

The technique of PIV was adapted to study the local deformation rates of hydrogel microstructures. In PIV, two images of “seed” particles are taken as they are transported by the motions of a fluid stream. With precise knowledge of the time separation between images and measurement of the distance that the particles have moved, it is then possible to determine the flow velocity. This procedure can be followed for small subsets of a larger image, producing a regular grid of velocity vectors, where each vector represents the average motion of the fluid particles in that portion of the flow field.

A PIV analysis of fluorescent particles trapped inside a hydrogel generates deformation rate vectors as the particles move with the hydrogel.^{28,29} The method of seed particle incorporation in the cylindrical hydrogel is identical to the method used to embed the larger glass beads in the tension samples discussed above. The seed particles used in PIV are two orders of magnitude smaller than the length scale of the hydrogel (1 μm particles in a 180 μm tall, 400 μm diameter gel cylinder) at a volume fraction of less than 1%. Smaller seed particles can also be used to further reduce this percentage, if experimental constraints required a smaller volume fraction.

A fluorescent microscope and a CCD camera are used to image the particles. All of the particles within the depth of

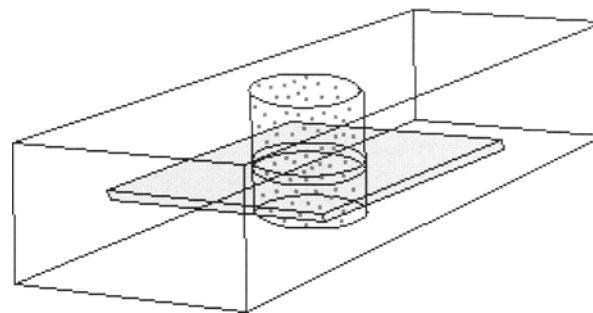


Fig. 9—Schematic diagram of a cylindrical hydrogel structure containing 1 mm diameter fluorescent seed particles. The shaded region signifies the depth of the measurement volume

focus of the microscope contribute to the image captured by the CCD camera (Fig. 9).³⁰ Therefore, the calculated velocity vectors represent the motion of the imaged particles within a volume bounded by the area of a grid spot and the depth of focus. A constant image-capture frequency achieved with either a pulsed laser or constant illumination and a shuttered exposure is used to acquire images. This technique allows valid measurements of the deformation rate of the hydrogel to be measured at various times during the expansion, by pairing the first image with a later image, such that the resulting time separation fits the required error constraints.³¹

Here we describe an investigation of the response of the hydrogel at two locations: where the hydrogel was in contact with the channel wall, and at mid-plane, halfway between the channel walls. At both locations, the volume change of identical cylindrical hydrogel posts, initially 400 μm in diameter and approximately 180 μm tall, were followed as they expanded in pH 12 solution. By focusing on two different planes of the hydrogel, it is possible to gain insight into the three-dimensional motions that exist during a volume expansion. An example of the type of information that can be derived from PIV is depicted in Figs. 10(a)–(f).

Discussion

Both sample preparation methods mentioned here provide versatile, efficient, and cost-effective means of producing test specimens. PDMS mold geometries can be modified easily and quickly with considerably less time and cost than is required in machining conventional molds. In addition, masking techniques allow microscale hydrogel structures to be created within complex channel configurations with the same geometrical latitude as the mold technique.

Although alternative techniques may be required to determine the functional properties of a hydrogel, tensile tests provide reliable data from which several material properties can be extracted. For instance, it is possible to determine ultimate strength, percent elongation at failure, Young’s modulus, and the Poisson ratio from a single tension test, whereas compression tests provide limited and qualitatively different information. Sample aspect ratios and frictional end effects must also be addressed if valid modulus measurements are to be obtained from compression testing.

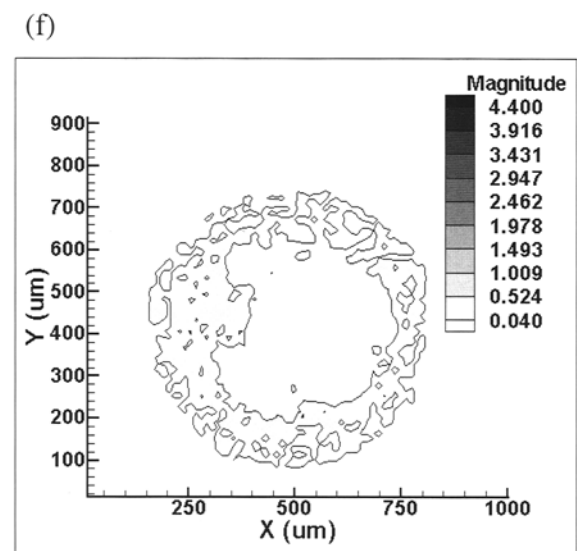
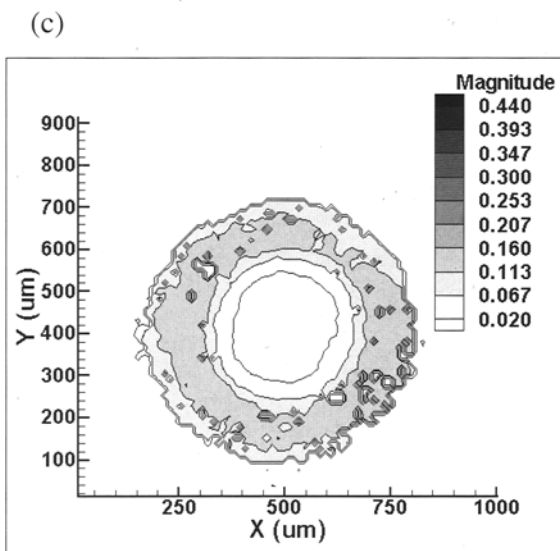
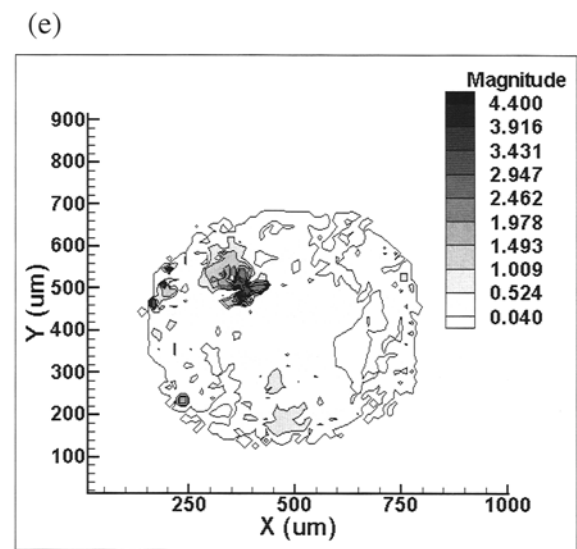
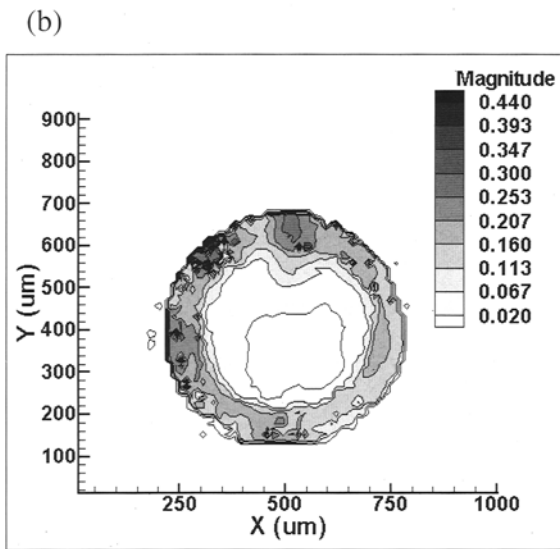
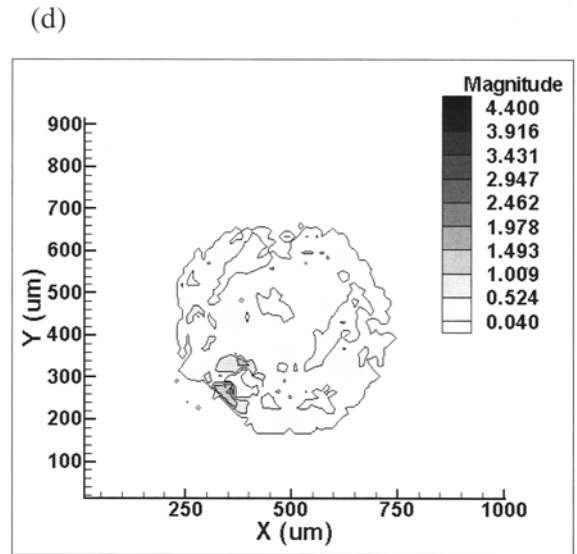
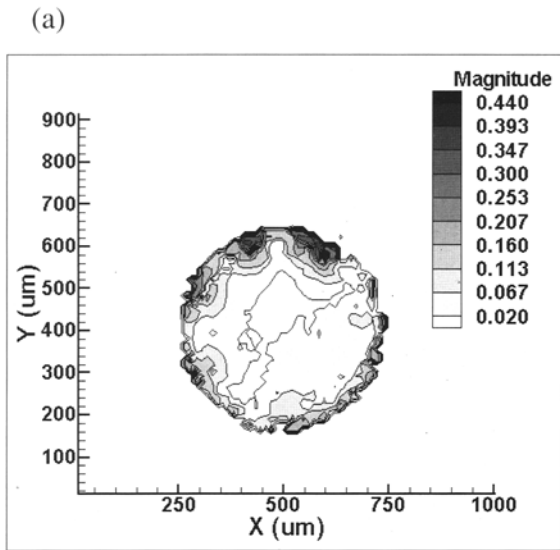


Fig. 10—Contour plots of the rate of expansion (mm s^{-1}) at the mid-plane (a)–(c) and top (d)–(f) of the structure at various times during the volume expansion: (a),(d) 20% completion; (b),(e) 40% completion; (c),(f) 60% completion

Ultimately, it is desired that smaller sizes of hydrogels be tested using the force response method, in order to accurately characterize the structures used in microfluidic devices. Commonly, hydrogels of 250 μm diameter and 200 μm height are employed.⁹ Testing at this scale requires a refined procedure so the smaller sizes can be accommodated. In addition to size changes, the impact of the initial state of the sample just prior to testing is being investigated. Another interesting measurement that can be taken from the force response tests is the relaxation after the peak load is reached. Along with the relaxation rate, the final equilibrium force is very important for many of the device designs that utilize the force generated by hydrogel actuators.

In addition to the research presented above, further investigation is required to determine the extent to which bead and seed particle inclusions affect the mechanical and functional swelling behavior, respectively. It has been assumed that the influence of inclusions is negligible in the experiments presented because of the small fraction of the total structure volume they occupy. The glass beads used in the tension samples comprised much less than 0.1% of the gage volume while the seed particles used for PIV involve less than 1% of the gage volume. Although this is a trivial fraction of the volume, a qualitative study is necessary to confirm the validity of this assumption.

One disadvantage to using the bead and seed inclusions arises out of the fundamental gel behavior. Since the glass beads are polymerized in the gel's contracted state, a cavity is formed around the bead after the gel undergoes the swelling process (Fig. 11). This may introduce optical effects as well as the possibility of bead movement during the test, which explains the increase in experimental error observed with increased swelling. This is illustrated in Figs. 6(a) and 6(b) where the strain data vary over a much wider range for samples tested in pH 12 solution as compared with samples tested in pH 2. A similar systematic increase in error was previously reported for tests conducted on swollen gel samples using ink markers to track the deformation in the sample.¹³ The increase in scatter was attributed to the fact that the ink tended to dissolve in the basic solution used to initiate swelling.

Another disadvantage arises in the limitations of the image acquisition system used for the Poisson ratio measurements. The test system performed adequately for the slow displacement rates used in this study. However, if an extensive study is conducted to determine the dependence of the Poisson ratio on strain rate, an alternative image acquisition system may be required.

For the PIV results, contour plots of the rate of expansion at two different planes show that the respective rates of deformation are not identical at a given time in the gel expansion process. One possible explanation for this behavior is that the unconstrained middle section of the hydrogel cylinder is expanding faster than the portion of the gel that is constrained through contact with the channel wall. Friction at the hydrogel/wall interface could produce this result as well as the relatively uneven rates of deformation at the interface, as compared to the middle section of the hydrogel. As seen in Fig. 10, local deformation velocities at the wall can be ten times as large as those in the middle of the gel. However, these movements at the hydrogel/wall interface (which could possibly be stick-slip behavior) are brief, and of much higher magnitude than the average expansion rate at the interface. At present, it is possible to state that the hydrogel experiences

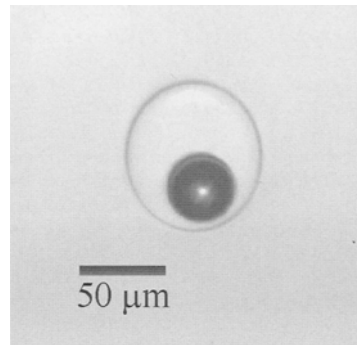


Fig. 11—Optical image of a 40 μm diameter bead in a cavity formed during the gel swelling process

different rates of expansion based on distance from an immobile solid surface that it is in contact with. Although only one plane can be imaged for a given expansion, it may be possible to reconstruct the results into a three dimensional picture of the hydrogel expansion.

Determining at what concentration, if any, the particles begin to affect the hydrogel expansion, checking the repeatability of measurements in a given plane, and imaging more cross-sections constitute further work that will more precisely define the limitations of the application of PIV to hydrogels and provide additional information on hydrogel dynamics.

Conclusions

A review of three techniques for testing the macroscopic uniaxial tensile properties and the functional swelling behavior of hydrogel structures in microchannels has been presented. Uniaxial tensile tests provide a means to determine a number of mechanical properties at different levels of swelling equilibrium. Quantification of the force generated by hydrogel actuators, as well as the rate of expansion in dynamic swelling was also demonstrated experimentally. Furthermore, novel methods of sample fabrication, permitting multiple samples to be created simultaneously with easily varied geometries, were also presented. The techniques outlined afford certain advantages as well as limitations in the testing and characterization of hydrogel behavior.

Acknowledgments

This research was sponsored by DARPA-MTO (F33615-98-1-2853) and DARPA, AFRL, Air Force Command, and USAF under agreement F30602-00-1-0570. The authors would also like to thank David Eddington, Glennys Mensing, and Jaisree Moorthy for helpful discussions and technical assistance.

References

- Osada, Y. and Rossmurphy, S.B., "Intelligent Gels," *Scientific American*, **268** (5), 82–87, (1993).
- Seigel, R.A., "Implantable, Self-Regulating Mechanochemical Insulin Pump," *The Regents of the University of California, Berkeley, CA* (1991).
- Tanaka, T., et al., "Phase Transitions in Ionic Gels," *Physical Review Letters*, **45** (20), 1636–1639, (1980).
- Grodzinsky, A.J. and Grimshaw, P.E., "Electrically and Chemically Controlled Hydrogels for Drug Delivery," *Pulsed and Self-Regulated Drug Delivery*, 47–64 (1990).

5. Tanaka, T., Nishio, I., Sun, S.T. and Uenonishio, S., "Collapse of Gels in an Electric Field," *Science*, **218** (4571), 467-469 (1982).
6. Hu, Z.B., Zhang, X.M. and Li, Y., "Synthesis and Application of Modulated Polymer Gels," *Science*, **269** (5223), 525-527 (1995).
7. Miyata, T., Asami, N. and Uragami, T., "A Reversibly Antigen-Responsive Hydrogel," *Nature*, **399** (6738), 766-769 (1999).
8. Beebe, D.J., Moore, J.S., Bauer, J.M., Yu, Q., Liu, R.H., Devadoss, C. and Jo, B.H., "Functional Hydrogel Structures for Autonomous Flow Control Inside Microfluidic Channels," *Nature*, **404** (6778), 588-590 (2000).
9. Liu, R.H., Yu, Q. and Beebe, D.J., "Fabrication and Characterization of Hydrogel-Based Microvalves," *Journal of Microelectromechanical Systems*, **11** (1), 45-53 (2002).
10. Ambrosio, L., De Santis, R., Iannace, S., Netti, P.A. and Nicolais, L., "Viscoelastic Behavior of Composite Ligament Prostheses," *Journal of Biomedical Materials Research*, **42** (1), 6-12 (1998).
11. Anseth, K.S., Bowman, C.N. and BrannonPeppas, L., "Mechanical Properties of Hydrogels and Their Experimental Determination," *Biomaterials*, **17** (17), 1647-1657 (1996).
12. Cauich-Rodriguez, J.V., Deb, S. and Smith, R., "Effect of Cross-Linking Agents on the Dynamic Mechanical Properties of Hydrogel Blends of Poly(Acrylic Acid)-Poly(Vinyl Alcohol Vinyl Acetate)," *Biomaterials*, **17** (23), 2259-2264 (1996).
13. Marra, S.P., Ramesh, K.T. and Douglas, A.S., "Mechanical Characterization of Active Poly(Vinyl Alcohol)-Poly(Acrylic Acid) Gel," *Materials Science and Engineering C-Biomimetic and Supramolecular Systems*, **14** (1-2), 25-34 (2001).
14. Muniz, E.C. and Geuskens, G., "Compressive Elastic Modulus of Polyacrylamide Hydrogels and Semi-IPNs with Poly(N-Isopropylacrylamide)," *Macromolecules*, **34** (13), 4480-4484 (2001).
15. Solari, M., "Evaluation of the Mechanical Properties of a Hydrogel Fiber in the Development of a Polymeric Actuator," *Journal of Intelligent Material Systems and Structures*, **5** (3), 295-304 (1994).
16. Stammen, J.A., Williams, S., Ku, D.N. and Guldberg, R.E., "Mechanical Properties of a Novel PVA Hydrogel in Shear and Unconfined Compression," *Biomaterials*, **22** (8), 799-806 (2001).
17. Zaroslov, Y.D., Philippova, O.E. and Khokhlov, A.R., "Change of Elastic Modulus of Strongly Charged Hydrogels at the Collapse Transition," *Macromolecules*, **32** (5), 1508-1513 (1999).
18. Ilavsky, M., "Phase-Transition in Swollen Gels .2. Effect of Charge Concentration on the Collapse and Mechanical-Behavior of Polyacrylamide Networks," *Macromolecules*, **15** (3), 782-788 (1982).
19. Dowling, N.E., *Mechanical Behavior of Materials*, Prentice-Hall, Englewood Cliffs, NJ, 135-136 (1998).
20. Johnson, B., Crone, W.C. and Beebe, D.J., "The Effects of Swelling on the Mechanical Properties of a pH Sensitive Hydrogel," *Materials Science and Engineering*, to appear.
21. Jo, B.H., Van Lerberghe, L.M., Motsegood, K.M. and Beebe, D.J., "Three-Dimensional Microchannel Fabrication in Polydimethylsiloxane (PDMS) Elastomer," *Journal of Microelectromechanical Systems*, **9** (1), 76-81 (2000).
22. Wallmersperger, T., Kroplin, B., Holdenried, J. and Gulch, R.W., "A Coupled Multi-Field-Formulation for Ionic Polymer Gels in Electric Fields," *Proceedings of the SPIE 8th Annual International Symposium on Smart Structures and Materials*, Newport Beach, CA (2001).
23. De, S.K., Ahuru, N.R., Johnson, B., Crone, W.C., Beebe, D.J. and Moore, J., "Equilibrium Swelling and Kinetics of pH-responsive Hydrogels: Models, Experiments, and Simulations," *Journal of Microelectromechanical Systems*, **11** (5), 544-555 (2002).
24. ASTM D 638-99, "Standard Test Method for Tensile Properties of Plastics," 46-58 (1999).
25. Johnson, B., Niedermaier, D.J., Crone, W.C., Moorthy, J. and Beebe, D.J., "Mechanical Properties of a pH Sensitive Hydrogel," *Proceedings of the 2002 SEM Annual Conference*, Milwaukee, WI (2002).
26. Eddington, D.T., Liu, R.H., Moore, J.S. and Beebe, D.J., "An Organic Self-Regulating Microfluidic System," *Lab on a Chip*, **1**, 96-99 (2001).
27. Trimmer, W., editor, *Micromechanics and MEMS: Classic and Seminal Papers to 1990*, IEEE, New York (1997).
28. Olsen, M.G., Bauer, J.M. and Beebe, D.J., "Particle Imaging Technique for Measuring the Deformation Rate of Hydrogel Microstructures," *Applied Physics Letters*, **76** (22), 3310-3312 (2000).
29. Bauer, J.M. and Beebe, D.J., "A Method for Measuring Deformation Rates in Hydrogel Structures: Multi-Plane Imaging and Measurement Limitations," *Proceedings of the 2000 International Mechanical Engineering Congress and Exposition*, Orlando, FL (2000).
30. Olsen, M.G. and Adrian, R.J., "Out-of-Focus Effects on Particle Image Visibility and Correlation in Microscopic PIV," *Experimental Fluids*, **29**, S166-S174 (2000).
31. Keane, R. D. and Adrian, R. J., "Theory of Cross-Correlation Analysis of PIV Images," *Applied Scientific Research*, **49**, 191-215 (1992).